Euro-Atlantic Atmospheric Circulation during the Late Maunder Minimum

Javier Mellado-Cano

Instituto Dom Luiz, Faculdade de Ciências, Universidade de Lisboa, Lisbon, Portugal

David Barriopedro

Instituto de Geociencias, CSIC-UCM, Madrid, Spain

Ricardo García-Herrera

Instituto de Geociencias, CSIC-UCM, and Departamento de Física de la Tierra II, Facultad de Ciencias Físicas, Universidad Complutense de Madrid, Madrid, Spain

Ricardo M. Trigo

Instituto Dom Luiz, Faculdade de Ciências, Universidade de Lisboa, Lisbon, Portugal

Mari Carmen Álvarez-Castro

Laboratoire des Sciences du climat et de l'Environnement/IPSL, CEA-CNRS-UVSQ, Université Paris-Saclay, Gif-sur-Yvette, France

ABSTRACT

This paper presents observational evidence of the atmospheric circulation during the Late Maunder Minimum (LMM, 1685–1715) based on daily wind direction observations from ships in the English Channel. Four wind directional indices and 8-point wind roses are derived at monthly scales to characterize the LMM. The results indicate that the LMM was characterized by a pronounced meridional circulation and a marked reduction in the frequency of westerly days all year round, as compared to the present (1981–2010). The winter circulation contributed the most to the cold conditions. Nevertheless, findings indicate that the LMM in Europe was more heterogeneous than previously thought, displaying contrasting spatial patterns in both circulation and temperature, as well as large decadal variability. In particular, there was an increase of northerly winds favoring colder winters in the first half of the LMM, but enhanced southerlies contributing to milder conditions in the second half of the LMM. The analysis of the atmospheric circulation yields a new and complete classification of LMM winters. The temperature inferred from the atmospheric circulation confirms the majority of extremely cold winters well documented in the literature, while uncovering other less documented cold and mild winters. The results also suggest a nonstationarity of the North Atlantic Oscillation (NAO) pattern within the LMM, with extremely cold winters being driven by negative phases of a "high zonal" NAO pattern and "low zonal" NAO patterns dominating during moderately cold winters.

1. Introduction

It is generally recognized that the Little Ice Age (LIA, ca. 1300–1900; e.g., Wanner et al. 2000) was one of the coldest periods in the last two millennia (e.g., Mann et al. 2009; Ljungqvist et al. 2012; Masson-Delmotte et al. 2013; PAGES 2k Consortium 2013; Kaufman 2014). This is based on evidences from proxy records of both hemispheres (mainly Europe, North America, and eastern China; Chambers et al. 2014), which strongly suggest that the LIA was a global phenomenon (Rhodes et al. 2012). Accordingly, almost all available reconstructions of the Northern Hemisphere agree that all 30-yr intervals from 1200 to 1899 were very likely colder than the 1983–2012 instrumental period (e.g., Masson-Delmotte et al. 2013). However, the timing and spatial

structure of the LIA are thought to be complex, exhibiting strong regional variations (e.g., D'Arrigo et al. 2006; Fernández-Donado et al. 2013; Schimanke et al. 2012). While the transition from the Medieval Climate Anomaly (MCA, ca. 900–1250) to the LIA has partially been attributed to changes in external forcings (e.g., Hegerl et al. 2011; Landrum et al. 2013; Schurer et al. 2013; Andres and Peltier 2016), internal feedback mechanisms (e.g., Lehner et al. 2013) and changes in atmospheric circulation (e.g., Goosse et al. 2012) must be also considered in order to explain the spatial heterogeneity and the regional signatures of the LIA.

The Maunder Minimum (MM, 1645–1715) is often regarded as the coldest period of the LIA (Luterbacher et al. 2001; Barriopedro et al. 2008) and was concurrent with an extremely low number of sunspots (Vaquero et al. 2016). The coldness reached its climax during the last decades of the MM, often called the Late Maunder Minimum (LMM, ca. 1685–1715; Wanner et al. 1995; Slonosky et al. 2001). The exceptionally low temperatures recorded across Europe make the LMM a period of great interest from a climatic viewpoint (e.g., Wanner et al. 1995; Luterbacher et al. 2001; Slonosky et al. 2001; Xoplaki et al. 2001; Xoplaki et al. 2005; Niedźwiedź 2010). The climatic information for this period comes from either early documentary sources or natural proxies (e.g., Pauling et al. 2006; McShane and Wyner 2011; Barboza et al. 2014), but the availability of proxies for the winter season is scarce and the instrumental evidence is limited to a small number of local historical series (e.g., Camuffo et al. 2010; Cornes et al. 2013). More recently, attention has turned to direct observations kept in documentary sources, which have higher temporal resolution than proxies (e.g., Garcia et al. 2001; Wheeler et al. 2010; Küttel et al. 2010; Lawrimore et al. 2011; Menne et al. 2012). In particular, marine meteorological data found in old ships' logbooks are a source of climatic information less exploited than observations in land, and have several assets (Wheeler and García-Herrera 2008; Wheeler 2014): 1) they provide first-hand and well-dated daily (sometimes subdaily) weather information back to the seventeenth century; 2) they cover the seas and oceans, for which the paleoclimatic information is scarce; and 3) although they have become a common source of information in the last years, most ships' logbooks are yet to be fully exploited.

Among all the information that ships' logbooks contain, wind direction taken aboard ships can be considered an instrumental observation, as it has been measured since the beginning of the twelfth century with a compass of 16 to 32 points (Jackson et al. 2000; Jones and Salmon 2005). Unlike indirect documentary information and other instrumental series, wind direction does not require subjective judgments or rescaling to modern quantitative standards. Wind direction has only recently been exploited for the study of past climate variability (e.g., Wheeler 2005; Gallego et al. 2007; Küttel et al. 2010), allowing researchers to build atmospheric circulation indices in different areas of the globe for the last centuries (e.g., Barriopedro et al. 2014; Ayre et al. 2015; Gallego et al. 2015; Ordóñez et al. 2016; Vega et al. 2018). These recent works have uncovered unprecedented climatic events, as for instance, an extremely wet period in the Sahel during the second half of the nineteenth century (e.g., Gallego et al. 2015). They have also stressed the added value of these observations to improve the skill of current reconstructions over Europe (Küttel et al. 2011).

Here, we present new instrumental evidence for the LMM consisting of daily observations of wind direction taken on ships since 1685 over the eastern Atlantic. While previous works have mainly focused on the analysis of a certain wind direction (e.g., the westerly index; Barriopedro et al. 2014; Vicente-Serrano et al. 2016), in this paper we adopt a more comprehensive view by considering simultaneously all wind directions in order to characterize better the atmospheric variability. The main objectives of the paper are twofold: first, to characterize the atmospheric circulation at monthly and seasonal scales during the period 1685–1715, including the interannual and interdecadal variability, and second, to assess its contribution to explain the anomalous LMM conditions over Europe. This paper is structured as follows: The data and methodology are described in section 2. Section 3 is devoted to the main results. Finally, conclusions are outlined in section 4.

2. Data and methodology

The English Channel (48°–52°N, 10°–5°E) has traditionally been a strategic route of intense marine activity, thus providing enough data density to derive nearly continuous series. Furthermore, previous studies have shown that this area, located at the exit zone of the extratropical jet stream, is representative of the circulation over most of the North Atlantic and consequently can be a good indicator of the European climate (Wheeler et al. 2010; Barriopedro et al. 2014; Vicente-Serrano et al. 2016; Kidston et al. 2015).

Daily wind records over the English Channel were abstracted for the LMM (1685–1715) from Royal Navy ships' logbooks kept in the National Maritime Museum and the U.K. National Archives (Wheeler et al. 2010). For each day of this period, only one (the midday) wind observation was kept. Herein, all wind direction

observations were corrected for the magnetic declination and referred to the true north by using the spatial-averaged monthly magnetic declination over the English Channel derived from the NOAA National Geophysical Data Center (NGDC) at $1° × 1°$ resolution (Jackson et al. 2000).

From 1901 on, the International Comprehensive Ocean–Atmosphere Data Set (ICOADS, version 3.0; Freeman et al. 2017) was employed as a benchmark for the LMM. ICOADS provides surface marine data from different sources, mainly ships (69.2%). The frequency of the daily ICOADS' observations within the English Channel increases with time, showing an abrupt growth in the last part of the record, largely due to wind observations taken at different times of the day over the same geographical locations (not shown). For coherence with the logbooks' observations of the 1685–1715 period, and to avoid biases toward oversampled points, we only selected the ICOADS' ships' observations that were closest to 12:00 UTC.

The resulting database includes calm and variable winds and has at least one record per day for most of the analyzed periods (96.0% and 93.2% of the days with observations in the LMM and in 1901–2014, respectively), except for some intervals during WWII. These observations have already been evaluated in previous studies for the period 1685–2008 (Wheeler et al. 2010; Barriopedro et al. 2014). For additional details on these datasets, the reader is referred to Wheeler et al. (2010), Barriopedro et al. (2014), and references therein.

To assess the atmospheric circulation during the LMM, two sets of monthly indices were derived from the daily wind direction records. First, considering the same rationale used for the "British Isles weather types," which provide a satisfactory insight into the synoptic circulation over the area (Lamb 1972), we computed four directional indices (DIs), one for each cardinal direction: northerly {NI, [315°–45°)}, easterly {EI, [45°, 135°)}, southerly {SI, [135°–180°)}, and westerly {WI, [225°, 360°)}. They are defined as the percentage of nonmissing days per month with wind blowing from that direction (calm and variable winds are excluded; Wheeler et al. 2010). To do so, we first classified each day by its prevailing wind direction, demanding a minimum percentage of daily observations with that wind direction. Following Barriopedro et al. (2014), this threshold is DI dependent (44%, 37%, 45%, and 36% for EI, SI, WI, and NI, respectively) in order to account for climatological differences in their frequency. The monthly DIs series were considered meaningful when more than two-thirds of the days in the month had at least one wind observation (otherwise, the month was labeled as missing). Figure 1 shows the wintertime series of the DIs for the LMM in standardized anomalies with respect to the 1981–2010 period, which contains the same number of years as the LMM, and will be used as a reference period, unless otherwise stated. This reduced number of indices allows us to interpret easily the main characteristics of the synoptic-scale circulation and the associated impacts in terms of temperature and precipitation. Thus, for example, an increased persistence of EI (WI) indicates dry (wet) advection from land (ocean), and the NI (SI) is related to cold (warm) advection from higher (lower) latitudes.

However, the wind direction data allow for a more detailed description of the atmospheric circulation than that derived from the DIs, which can be useful in order to provide a better interpretation of extreme events and the underlying dynamics involved in specific episodes. Thus, in addition to the 4-point DIs, monthly 8-point (45°) wind roses were derived from the mean wind direction of each day. For coherence with the DIs, the 8-point wind roses are constructed in 45° bins starting at 0° such that each DI corresponds to two full bins in the wind rose.

3. Results

a. Mean atmospheric circulation for the LMM

Figure 2 shows the seasonal DIs averaged for the LMM (1685–1715, color bars) and compares them with those of the reference period (1981–2010, gray bars). For both periods, the WI is the most recurrent DI, indicating the predominance in the region of westerly winds. Also, in both periods, the WI displays a pronounced annual cycle, with a maximum in summer, contrasting with the less pronounced seasonality of the SI, which presents a winter maximum. The frequency of days with meridional circulation (the sum of SI and NI) during the LMM was slightly higher than during the reference period, and the WI presented lower frequencies in the LMM than in the reference period for all seasons. As shown by Barriopedro et al. (2014), a below-normal persistence of westerlies inhibits the warm oceanic advection over most of Europe during all seasons, except in summer, when it is rather associated with high-pressure systems and radiative warming. In terms of precipitation, the WI is an optimal indicator of the transport of moisture fluxes to Europe, with decreased westerlies denoting below-average precipitation over large areas of central Europe all year round (Barriopedro et al. 2014). Accordingly, the reduced frequency of WI in Fig. 2 indicates a drier and colder LMM compared to present (with the exception of summer). The remaining DIs have also robust
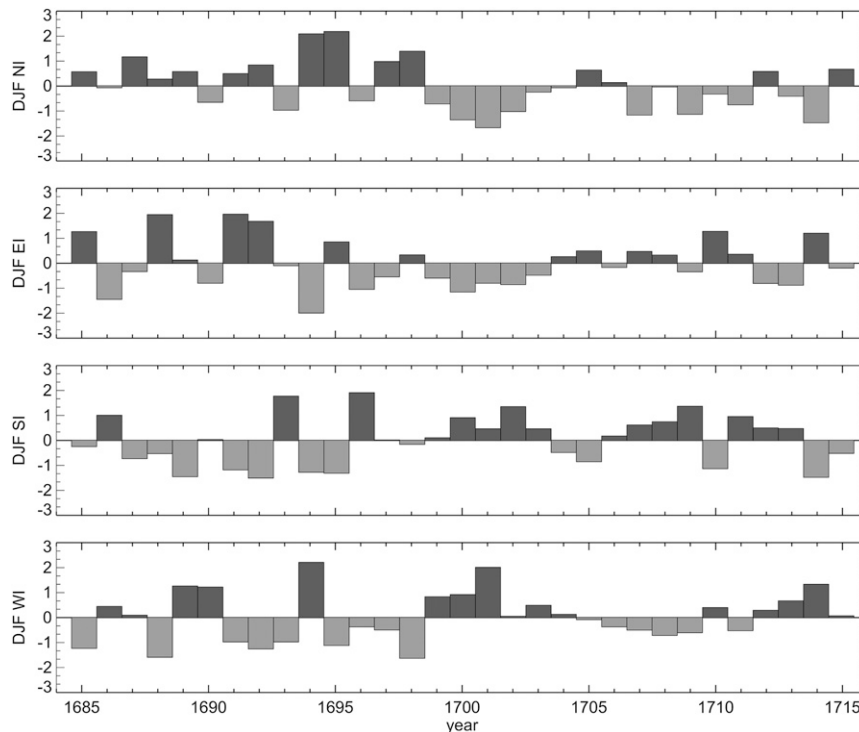
FIG. 1. Standardized winter DIs time series for the LMM (1685–1715), with dark (light) gray
bars highlighting years with values above (below) the 1981–2010 avg.

temperature responses over large areas of Europe (not shown). More specifically, there is a tendency for the EI and NI (SI) to be associated with cold (warm) temperature anomalies, particularly in winter and over central and western Europe.

Seasonally, summer and winter are the seasons of the LMM that show the largest (significant) differences with the reference period (Fig. 2). Therefore, in the following analyses, we will focus on these seasons. Winters were characterized by a low frequency of westerlies and high values of northerlies, both contributing to a pronounced cooling due to the reduction (intensification) of warm (cold) advection from the ocean (higher latitudes). Differently, LMM summers exhibited a low frequency of westerlies and increase of southerlies. Together, these anomalies tend to favor warmer temperatures. Note that in both cases, the reduced westerlies lead to more extreme seasons, with less influence of oceans. Hence, on average, the role of the atmospheric circulation on European temperature displayed a clear seasonal contrast: in winter, the dynamics favored cold conditions in Europe, while in summer it promoted warm conditions. However, it is worth noticing that the effects of the atmospheric circulation on European temperatures are weaker in summer than in winter because of the smaller pressure gradients over the North Atlantic and the

higher contribution of regional and thermodynamical processes (Vautard and Yiou 2009). In agreement with that, the temperature fingerprints of the DIs extend over larger European areas in winter than in summer (e.g., Barriopedro et al. 2014).

Overall, the values of the DIs during the LMM do not seem exceptional when compared with those of the reference period (1981–2010; Fig. 2) or the twentieth century (1901–2014; not shown). This contrasts with the extreme temperature character of the LMM. This apparent decoupling between the atmospheric circulation and the surface conditions could be partly explained by an enhanced role of thermodynamical processes associated with changes in the external forcings, such as volcanism and solar activity, similar to what has been reported for the last decades of increasing anthropogenic forcing (Vautard and Yiou 2009). Notwithstanding, many studies stress the necessity to account for the large-scale dynamics when assessing the climatic impact of solar variability (e.g., Barriopedro et al. 2008) or major volcanic events, such as the outstanding eruption of Tambora in 1815 (e.g., Trigo et al. 2009; Luterbacher and Pfister 2015). Changes in atmospheric circulation, either internal or externally forced, are also necessary to explain the spatial heterogeneity and the extreme character of specific events that occurred during the
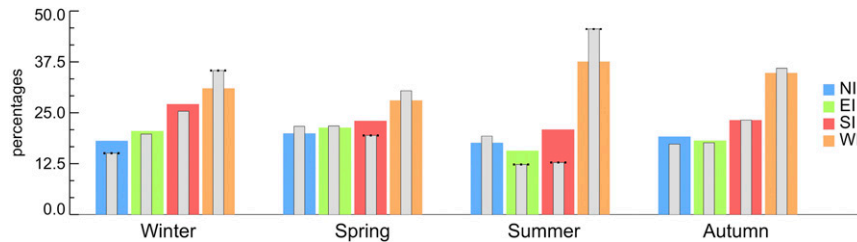
FIG. 2. Seasonal frequencies of DIs (in percentage of total days) averaged for the LMM (color bars). Gray thin bars indicate the corresponding value for the 1981–2010 reference period. Gray bars with dotted tops indicate significance diff between the two periods at the 90% confidence level after a two-tailed *t* test.

LMM (Alcoforado et al. 2000; Niedźwiedź 2010). In this sense, our results indicate that the atmospheric circulation contributed to the cold European temperatures of the LMM during winter. By contrast, the summer circulation anomalies were prone to mild conditions, and at most they acted to offset any expected radiative cooling that can be attributed to changes in external forcings. This is in agreement with previous studies, which have stressed that the cold conditions of the LMM were essentially confined to winter (e.g., Wanner et al. 1995; Luterbacher et al. 2001; Slonosky et al. 2001). In consequence, in the remainder of the paper we will focus on the LMM circulation during winter and the associated temperature responses. More specifically, we will address the variability of the atmospheric circulation within the LMM, from intraseasonal to interdecadal time scales.

b. Intraseasonal to interdecadal variability

To address intraseasonal changes within the LMM, we computed the mean LMM wind roses for each calendar month of the winter season, that is, December, January, and February. Overall, the results are consistent with the behavior shown by the winter DIs in Fig. 2 (i.e., enhanced NI and reduced WI), and display an overall resemblance during all winter months, indicating sustained anomalies through the winter season (Fig. S1 in the supplementary information). Thus, LMM winters were characterized by statistically significant increased frequencies in the NE and/or NW directions, as compared to the reference period. On the other hand, the SW component stands out by its reduced frequency through all winter months. Although the wind roses uncover additional information to that provided by the DIs, still, on average, they do not show exceptional anomalies for any wind direction and month. This suggests that the extremely cold conditions may have arisen from the combined effect of simultaneous anomalies affecting to different wind directions.

With the aim to explore the decadal variability, we divided the winters of the LMM into two subperiods of approximately equal length (1685–99, first half; 1700–15, second half). The wind roses of the two halves are superimposed on Fig. 3, with blue and red shading indicating a larger predominance of that wind direction in the first and second half of the LMM, respectively. The winter wind roses reveal remarkable decadal changes in circulation. The increased frequency of northerly and easterly winds that characterized the first half of the LMM was replaced by opposite anomalies (enhanced southerly and westerly winds) in the second one. Overall, these interdecadal changes in circulation are observed in all winter months, notably during December and January, and suggest that the first half of the LMM was much colder than the second one. An example of the substantial decadal winter variability within the LMM is found in the 1690s decade, which, on average, was dominated by increased northerlies and reduced westerlies (standardized DIs anomalies of $NI_{\overline{1690s}} = 0.36$; $EI_{\overline{1690s}} = 0.10$; $SI_{\overline{1690s}} = 0.20$; $WI_{\overline{1690s}} = -0.41$). The predominance of the cold advection from northerly and easterly winds over the warm advection associated with westerlies and southerlies confirms the cold conditions reported by previous authors (e.g., Luterbacher et al. 2001; Niedźwiedź 2010). As an exception to this cold decade, the 1699 winter was mild (Luterbacher et al. 2001; Alcoforado et al. 2000; Slonosky et al. 2001; Barriopedro et al. 2014), in agreement with an increased persistence of westerlies and southerlies ($NI_{1699} = -0.65$; $EI_{1699} = -0.42$; $SI_{1699} = 0.46$; $WI_{1699} = 0.36$). The analysis of the two LMM halves allows us to conclude that the large interdecadal winter variability within the LMM should be taken into account to explain the relatively weak circulation anomalies observed for the entire LMM in Fig. 2. Moreover, the seasonal DIs are able to capture episodes of shorter duration (e.g., 1699) and hence the interannual variations of the atmospheric circulation during the LMM. Therefore, in the remaining sections, we will focus on characterizing the interannual variability of the
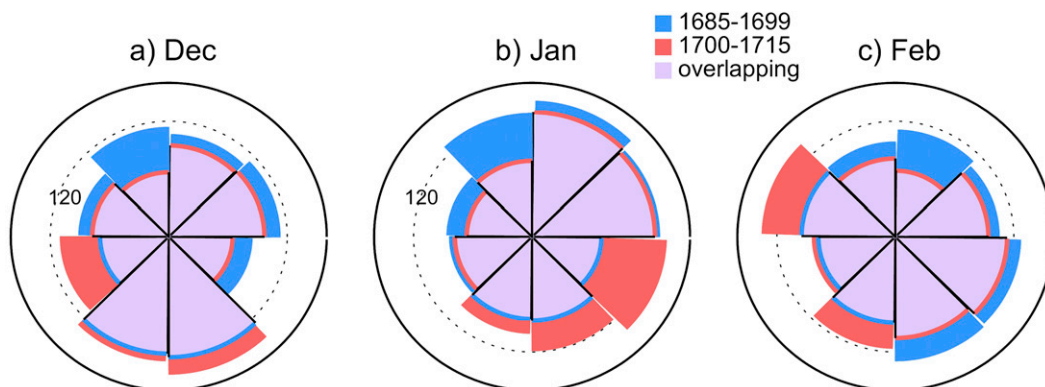
FIG. 3. Monthly mean 8-point wind roses for the first (1685–99, blue) and second (1700–15, red) half of the LMM: (a) December; (b) January; (c) February. Purple indicates the overlapped areas between both subperiods. For a better comparison, the frequency of each bin is expressed in percentage of normals with respect to 1981–2010 (contour interval of 40%).

LMM, and providing a detailed description of the LMM winters.

c. Interannual variability

To characterize the interannual circulation variability within the LMM and synthesize the four-dimensional information of the DIs, we computed a cumulative circulation index (CI) that aggregates the standardized values of the four DIs in two components (CI_x, CI_y):

$$CI_x = WI + SI - NI - EI \qquad (1)$$
$$CI_y = NI + SI - EI - WI. \qquad (2)$$

The component CI_x is purely based on atmospheric circulation, but it can also be used as an indicator of the European temperature conditions that could be expected from the dynamics, with positive (negative) values of CI_x indicating an overall warming (cooling). CI_y measures the degree of meridional (NI, SI) versus zonal (WI, EI) circulation, with positive (negative) values indicating a dominance of the former (latter).

Figure 4a shows the scatterplot of the CI components for the individual winters of the LMM. Overall, the results confirm that the meridional circulation (winters that are above zero in the y axis, $CI_y > 0$) predominated overwhelmingly during the LMM. In fact, only 19% of winters displayed a predominant zonal circulation anomaly (winters below the zero y axis, $CI_y > 0$). By contrast, on the 1981–2010 reference period, half of the winters were dominated by prevailing zonal circulation anomalies (see Fig. S2). By construction, the location of each winter along the x axis of the scatterplot in Fig. 4a is informative about the balance between wind components that promote cold advection $(CI_x < 0)$ from higher latitudes (NI) and the continent (EI), and

those associated with warm advection $(CI_x < 0)$ from the ocean (WI) and lower latitudes (SI). For example, the 1698 winter, at the upper-left corner $(CI_x = -2.74, CI_y = 2.26)$, was characterized by the prevalence of meridional (NI + SI) over zonal (WI + EI) flow, and of the cold (NI + EI) over the warm (WI + SI) advection $(NI_{1698} = 1.10; EI_{1698} = 0.44; SI_{1698} = 0.20; WI_{1698} = -1.40)$. Thus, during winters located at the right x axis, the dynamic is expected to favor warmer conditions because of a predominant southerly and westerly circulation, while winters placed on the left are prone to colder conditions as a result of dominant easterly and northerly winds. This is confirmed by a composite analysis of near-surface temperatures for winters of the reference period that were stratified by CI_x into winters with $CI_x > 0$ and winters with $CI_x > 0$ separately (Fig. S3). Attending to CI_x, the results of Fig. 4a reveal two different groups of winters, located in the left $(CI_x < 0)$ and right $(CI_x < 0)$ x axis, respectively. The color of the symbols in the scatterplot represents the year of each LMM winter, and its distribution indicates that these two groups tend to organize in the first and second half of LMM, respectively. This confirms the high decadal variability during the LMM, with a first half colder than the second one.

To confirm that the two groups of winters identified in Fig. 4a actually display different circulation anomalies in terms of the DIs, we applied a k-means clustering analysis (Wilks 2006) to the four DIs of the 31 LMM winters. This objective technique groups winters with similar distributions of DIs anomalies (i.e., with similar circulation signatures), and requires specifying a predefined number of clusters. When two clusters are set, it is found that the first cluster represents winters with anomalously high values of NI and EI, as revealed by the DIs values of its centroid
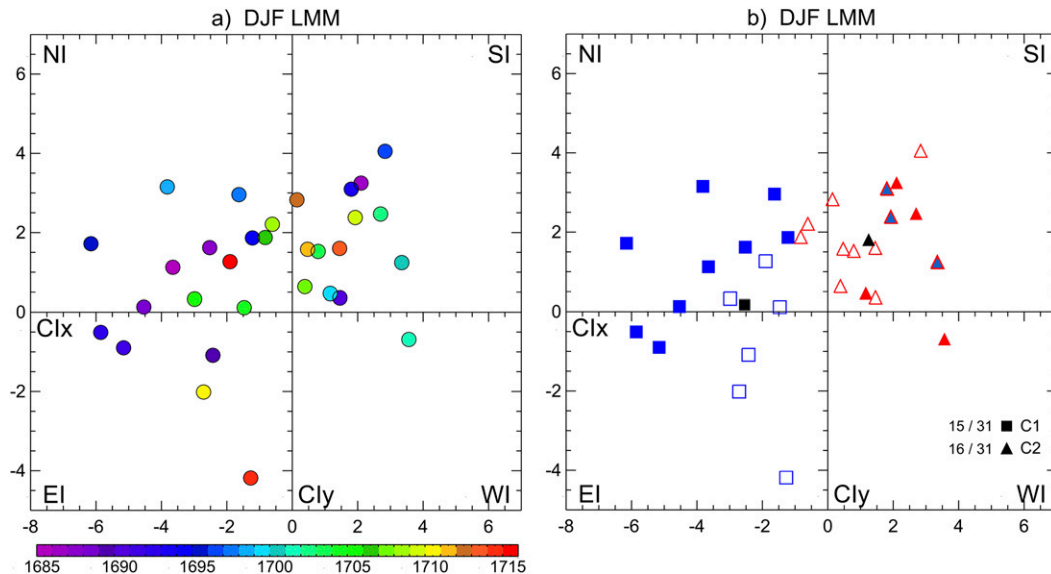
FIG. 4. (a) Scatterplot of the CI for the LMM winters, with colors indicating the year within the LMM. The *x* axis (*y* axis) represents the CI_x (CI_y) coordinate of the CI. (b) As in (a), but with open blue squares (red triangles) representing winters of the cluster one (two). The number of winters of each cluster is shown in the lower-right corner. Black symbols denote the centroid CI values of the cluster one (black square; $CI_x = -2.55$; $CI_y = 0.17$) and two (black triangle; $CI_x = 1.25$; $CI_y = 1.81$). Symbols filled with blue (red) in (b) represent well-documented cold (warm) winters in the literature. See text for details.

(EI = 0.42, SI = −0.77, WI = −0.41, NI = 0.95). On the other hand, winters belonging to the second cluster are dominated by positive anomalies of SI (centroid values of EI = −0.36, SI = 1.17, WI = −0.31, NI = −0.03). We stress herein that the cluster analysis only takes into account the information of the DIs, and hence the resulting classification of winters is based on dynamical arguments only. This analysis is also independent of that performed in Fig. 4a with the CI. However, Fig. 4b reveals that when the winters of each cluster are displayed in the CI scatter, the clusters tend to group according to CI_x. Accordingly, winters of the first cluster (blue squares in Fig. 4b) are preferably located in the left *x* axis ($CI_x < 0$) and coincide fairly well with the cold-prone winters of the first half of the LMM (Fig. 4a). On the contrary, winters of the second cluster (red triangles in Fig. 4b) tend to fall into the right side of the scatterplot ($CI_x < 0$), including the majority of the mild-prone winters of the second half of the LMM. Thus, the cluster analysis provides an objective tool to catalog winters of the LMM according to their circulation signatures, from which the dynamically driven temperature anomalies can be estimated and contrasted with independent studies.

d. New catalog of winters for the LMM

In this section, we address how well the temperature conditions inferred from the atmospheric circulation

compare with those reported elsewhere in order to evaluate the dynamical contribution to the LMM winter cooling. Filled symbols in Fig. 4b represent anomalous winters that have been well documented in the literature, based on multiple and independent evidences across Europe (see sources in Table S1 of the supplementary information). All of them were reported as cold (filled blue), except 1686, 1699, 1701, and 1702, which have been described as warm winters (filled red) in many regions of Europe. Note also that most well-documented cold winters occurred in the first half of the LMM and belong to our first cluster (blue squares in Fig. 4b). On the other hand, the few winters that have been documented as warm in the literature fall in our cluster two (red triangles). This general agreement provides an observational support to previous studies on cold winters, further stressing the major role of the atmospheric circulation in driving the variable conditions within the LMM. For the sake of simplicity, and in the following analyses, winters of the first and second cluster will also be referred to as dynamically cold and dynamically mild winters, respectively. However, we stress that this terminology relies on dynamical arguments only.

From Fig. 4b we also note that, to our knowledge, a substantial number of LMM winters have not been so well described in the literature (open symbols), with the exception of some reports, mainly confined to specific

locations, such as those by Kington (2010) for London. In this sense, the information provided by the DIs allows us to derive new observational-based evidences about the winter conditions of the LMM. To do so, we assigned each winter of the LMM to the first (dynamically cold) or the second (dynamically mild) cluster, according to their dynamical signatures (Fig. 4b). We then cross-referenced this catalog of LMM winters with evidences provided by the literature (Table S1) in order to assess the degree of agreement between the temperature anomalies expected from the atmospheric circulation and those reported elsewhere. This comparison allowed us to identify four groups of winters in the LMM, as shown in the last column of Table S1: (i) Group 1 (G1): dynamically cold winters cataloged as cold in other studies (1685, 1687, 1688, 1691, 1692, 1694, 1695, 1697, and 1698);(ii) Group 2 (G2): dynamically cold winters that have not been widely documented in the literature or whose evidence of cold conditions is spatially and/or temporally restricted (1689, 1704, 1705, 1710, 1714, and 1715);(iii) Group 3 (G3): dynamically mild winters that have been either reported as mild in the literature or at least not reported as cold (1686, 1690, 1696, 1699, 1701, 1702, 1703, 1706, 1707, 1708, 1711, 1712, and 1713); and (iv) Group 4 (G4): dynamically mild winters that have been described as cold in the literature (1693, 1700, and 1709). Note that G2 and G3 include some winters that, to our knowledge, have been less described or almost unnoticed so far, and for which the DIs provide supporting or new observational-based evidence.

To confirm the aforementioned heterogeneity of winters, and to explain discrepancies with previous studies, we have inferred the spatial pattern of temperature anomalies from the atmospheric circulation for each winter of the LMM. To do so, we first searched for the circulation analog of each winter of the LMM, among those available for the period 1901–2014. The analogs of circulation are calculated using the seasonal 8-point wind roses, which provide higher resolution and hence more detailed information of the atmospheric circulation than the four DIs. The analog of each LMM winter is the winter of the period 1901–2014 that minimizes the root-mean-square difference (RMSD; e.g., Vautard and Yiou 2012) of their wind roses. The spatial temperature and geopotential anomaly pattern of each LMM winter is the one corresponding to its "modern" analog.

The temperature and geopotential height fields have been obtained from the Climate Research Unit (CRU TS3; Harris et al. 2014), which is available at $0.5° \times 0.5°$ spatial resolution, and from the Twentieth Century Reanalysis, version 2c (20CR; Compo et al. 2011), at $2° \times 2°$ spatial resolution, respectively. As we are

exclusively interested in the temperature anomalies induced by the atmospheric circulation, the 1901–2014 linear trend of the seasonal temperature series was removed for each grid point before computing the temperature anomaly (with respect to the period 1981–2010). For coherence with the temperature field, we also removed the linear trends of the winter geopotential height. We stress that the method of analogs provides the temperature responses due to circulation anomalies, which in turn may have been internally or externally forced, but it does not account for temperature changes associated to other factors. In spite of this, previous studies have demonstrated a reasonable skill of the analog method in temperature reconstructions (e.g., Gómez-Navarro et al. 2017). The validation of the method is assessed by the mean-squared skill score [MSSS; Eq. (2)], which measures for each grid point the improvement of the forecast as compared to a climatological prediction (Wilks 2006):

$$ \text{MSSS} = \left(1 - \frac{\text{MSE}}{\text{MSEC}}\right)100, \tag{3} $$

where MSE and MSEC represent the mean-squared errors based on the selected analog and the climatological predictions, respectively. The significance of the MSSS was tested with a 5000-trial bootstrap method, by selecting randomly sets of observed and predicted values.

Taking the analogs as surrogates of the LMM winters, we derived the composite of temperature and geopotential height at 500-hPa anomalies for each group of LMM winters. Figure 5 shows the temperature and geopotential anomaly patterns for the winters of G1, G2, and G3. The composite for G1 (well-documented cold winters; Fig. 5a) shows a pronounced and widespread cooling across Europe, supporting the extreme conditions reported by independent sources (Table S1). Using historical series from different European regions, the mean temperature of these winters was 2.3°C for the central England temperature (CET; Manley 1974) and −0.1°C in the Netherlands (Van den Dool et al. 1978). The associated circulation displays a strong negative phase of the North Atlantic Oscillation (NAO) (e.g., Hurrell 1995; Jones et al. 1997), and shows a large resemblance to the unusual winter of 2009/2010 (Cattiaux et al. 2010; Ouzeau et al. 2011), which has been cataloged as the coldest winter of the last 100 years in some parts of Europe (Prior and Kendon 2011). Using the seasonal NAO index (Hurrell et al. 2003) for the analog winters of G1, we obtained an average value of −2.21 SD, in agreement with the circulation pattern of Fig. 5a.
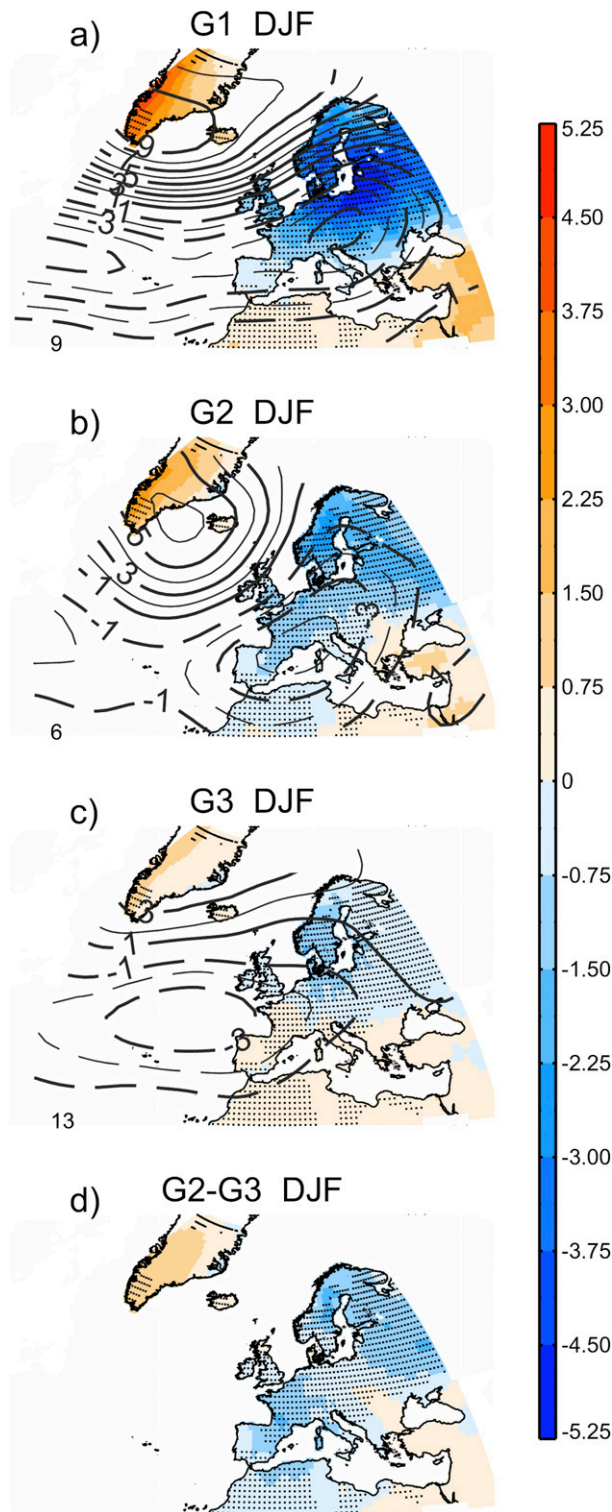
FIG. 5. Winter composites of near-surface temperature (shading, in °C) and geopotential height at 500-hPa (contours, in dam) anomalies for the winter analogs of: (a) G1; (b) G2; (c) G3; (d) the diff between G2 and G3. Dotted areas highlight those regions where the MSSS is significantly above the climatology at the 90% confidence level. Numbers at the left bottom of each panel indicate the total number of winters of each group.

The winters of G2 (dynamically cold winters with more limited evidences) were less extreme than those of G1, especially in central and northern Europe, but still cold throughout most of the continent (Fig. 5b). The instrumental series of temperature from central England (the Netherlands) give an average value of 3.6°C (2.3°C), which is higher than that obtained for G1 winters. The associated circulation was also characterized by a negative NAO-like pattern. However, and different to G1, the G2 pattern displays a departure of the NAO dipole from zonality with a migration of the centers of action. Interestingly, this "low zonal" NAO dipole reflects the dominant mode of variability during periods of decoupling (i.e., insignificant correlations) between the WI and the NAO, such as 1871–1900 (Barriopedro et al. 2014), while the corresponding pattern of G1 fits well into the "high zonal" NAO pattern, characterized by strong correlations between the WI and the NAO (e.g., 1901–30). These results support previous studies that have identified a variety of dominating circulation patterns during the LMM, with different frequencies of occurrence between its early and late stage (e.g., Luterbacher et al. 2001). The lack of stationarity in the NAO pattern described herein has not been clearly reported before, probably because of the inherent limitations of the proxy-based reconstructions of the NAO, thus reinforcing the added value of the wind direction data. The less extreme cold temperatures associated with the "low zonal" NAO pattern of G2 could be the reason for the more limited cold evidences of these winters.

The composite for G3 (dynamically mild winters with no clear evidences of coldness) confirms that these winters were not as cold as those of G1 or G2 (Fig. 5c). Indeed, the Mediterranean Basin displays relatively warm conditions, while a weak cooling signal is confined to northern and eastern European regions. The temperature pattern inferred from the atmospheric circulation is in good agreement with the instrumental series from central England (the Netherlands), which indicate mean temperatures of 4.3°C (3.1°C), higher than those obtained for G1 and G2. The difference between the composites of G3 and G2 (Fig. 5d) confirms that the winters of G2 were also colder than those of G3, emphasizing the large variability within the LMM. The circulation anomaly during the winters of G3 displays anomalous centers that are displaced southeastward with respect to the NAO, similar to the positive phase of the east Atlantic (EA) pattern (Barnston and Livezey 1987). We stress that G3 (and to some extent G2) contains winters that have not been extensively cataloged to date or whose evidence is restricted in spatial or temporal scales. Therefore, our analysis is particularly

informative of nonextreme winters (G2 and G3), for which documentary records often do not provide sufficient information.

Finally, we assess the winters of G4 (1693, 1700, and 1709), which are classified as dynamically mild winters herein, but have been documented as cold winters elsewhere. Note that the causes of the discrepancies could lay on the side of the proxies (e.g., evidences confined or biased to specific regions or seasons), our indices (e.g., a more limited skill to capture atmospheric circulation anomalies over regions far from the English Channel), or the methodology (e.g., inferential approach from a limited sample or the lack of good flow analogs). However, it could also indicate a reduced control of the dynamics on temperature (e.g., an enhanced role of external forcings). To clarify these discrepancies, we analyzed in more detail the winters of G4 by evaluating their analogs separately (Fig. 6). Different to the composite analysis of Fig. 5, the assessment of individual winters leads to noisier and more extreme fields than those obtained therein. Thus, to account for the range of temperature anomalies that can be obtained under the same atmospheric circulation and to avoid misleading comparisons with Fig. 5, we selected the analogs of each winter of G4 (up to a maximum of three) that do not double the RMSD of the best analog, and their average is shown instead. This choice was taken as a compromise between a low number of analogs, which can lead to nonrobust patterns, and high number of analogs, whose averaging can miss the extreme character of the winter.

The wind roses of 1693 (Fig. 6a) and 1700 (Fig. 6b) reveal higher values of the meridional wind components in both cases. The high frequency of southerly winds explains why these winters are cataloged as dynamically mild, with 1693 (1700) displaying 41% (30%) of days with wind blowing from 135° to 225°. Despite the overall cooling reported in previous studies, there are local evidences of coldness as well as warmness in some parts of Europe, suggesting heterogeneous regional patterns. Thus, the 1693 winter has been reported as cold and slightly cold in Iberia (Alcoforado et al. 2000) and Hungary (Rácz 1994), respectively. However, warmer or normal conditions were reported in Czech Republic (Brázdil et al. 2008), London (Kington 2010), and Switzerland (Pfister 1992). Based on the historical series of temperature, the 1693 winter was the 11th (7th) warmest winter of the 1685–1715 period in central England (the Netherlands). On the other hand, the reported cooling of the 1700 winter is mostly based on local evidences from Czech Republic (Brázdil et al. 2008), the Balkans, and Greece (Xoplaki et al. 2001), but there were near-normal temperatures in London
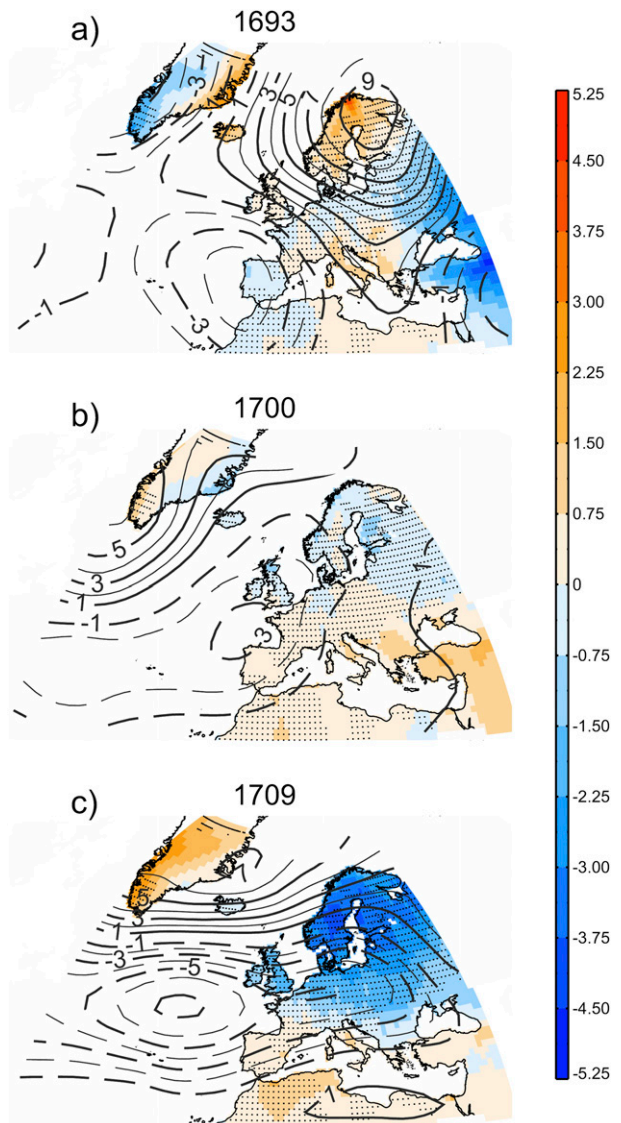

FIG. 6. As in Fig. 5, but for the avg of the best analogs of each winter of Group 4: (a) 1693; (b) 1700; (c) 1709. See text for details.

(Kington 2010) and Switzerland (Pfister 1992), and it was the third warmest winter of 1685–1715 in the Netherlands. In agreement with the literature, our results also suggest that the winter of 1693 (1700) was relatively cold in several European regions, including Iberia and Hungary (Czech Republic, Balkans), and warm in Czech Republic (the Netherlands). Regarding the atmospheric circulation, the analog winters of 1693 are dominated by a primary high-pressure center over Scandinavia, resembling a positive phase of the Scandinavia pattern (SCAND; Barnston and Livezey 1987), and a low-pressure center over Iberia, which may explain the reported cooling therein. On the other hand, the 1700 analogs are characterized by a negative phase

of the NAO, but with its centers displaced westward, especially the high-pressure anomaly, which is retreated toward Greenland, reducing the cold advection over the continent. In summary, the 1693 and 1700 winters featured a strong meridional circulation (including northerly and southerly components), thus likely leading to a heterogeneous spatial pattern with regional signals of warming and cooling across Europe, similar to the mild winters of G3 (Fig. 5b), but still compatible with indirect evidences reporting local or regional cold conditions.

Similar to the other winters of the G4, the 1709 winter (''The Great Frost,'' as it was known in England) displayed persistent northerly winds and hence it was actually cold in many areas of Europe (Fig. 6c). However, different to 1693 and 1700, the coldness of this winter is very well documented across Europe (Table S1). Thus, we investigated thoroughly the associated circulation by taking advantage of the daily resolution of our data. We found that December and February of 1709 were characterized by westerlies and southerlies, with the exception of some persistent intrusions of polar and continental winds, mainly in February. Accordingly, our data suggest a near-normal December and a cold February, which agrees with previous studies (Luterbacher et al. 2004; Kington 2010). As for January 1709, it has been reported as the coldest month of that winter in Europe (e.g., Luterbacher et al. 2004 and references therein), which is the main reason for discrepancy with our data. A detailed analysis of the daily wind direction observations revealed an important gap between 5 and 14 of January 1709. This is the only month of the LMM containing a long interval of successive missing days, while still satisfying the minimum threshold of available daily data to consider it as a nonmissing month. Unfortunately, this lack of data matches with an extremely cold polar outbreak in Europe, which started between 4 and 6 of January 1709 in England and France, and persisted until the middle of that month (Derham 1708; Maraldi 1710; Monahan 1993; Kington 2010). This period should have coincided with persistent northerly winds, likely changing the temperature character of January 1709 and the entire winter of 1709 to dynamically cold. Therefore, the discrepancy with the reported evidences can be attributed to a 10-day spell of missing data that is unique in our record, and hence the winter of 1709 should be reclassified as dynamically cold. In spite of this, the regional cooling reported in Greece and the Balkans (Xoplaki et al. 2001) is confirmed by our results (Fig. 6c). This result highlights the importance of daily data when explaining extreme events such as the winter of 1709.

Overall, our results indicate that the LMM was cold (see the LMM mean temperature pattern in Fig. S4a), but displayed substantial variability, both in atmospheric circulation and temperature. We note in closing that wind direction has also significant signals in precipitation across Europe (e.g., Barriopedro et al. 2014) and hence the wind roses can also be used to infer the anomalous precipitation patterns associated to the LMM. Accordingly, we have applied the same analysis of analogs to precipitation fields extracted from the Global Precipitation Climatology Centre (GPCC; Schamm et al. 2014) for the 1901–2014 period. Bearing in mind our approach, the results suggest that the LMM was overall a dry period (Fig. S4b), partially because of the reduced frequency of westerlies (the DI with the largest precipitation responses). However, the precipitation anomalies and decadal variability were not as large as in the case of temperature. We hypothesize that the reduced frequency of southerlies (easterlies) in the first (second) half of the LMM partially compensated for the precipitation deficits induced by the lack of westerlies.

4. Conclusions

In this paper, we present a new observational analysis of the LMM (1685–1715) based on direct instrumental evidence of the daily atmospheric circulation over the eastern Atlantic derived from wind direction observations taken aboard ships over the English Channel. We construct two sets of monthly atmospheric circulation indices that measure the persistence of the wind direction in the four cardinal directions and in 8-point wind roses, allowing us to explore the variability of the atmospheric circulation in a wide range of time scales (from monthly to decadal). These observational indices help to fill the gap of climate reconstructions, which often suffer from the scarcity of proxies for winter (Jones et al. 2014). Our study goes into more detail than earlier ones, and produces a new classification encompassing every winter between 1685 and 1715. The main findings can be summarized as follows:

- The LMM was characterized by a strong meridional circulation, with a generalized frequency reduction of the westerlies all year round, contributing to relatively cold and dry conditions in Europe. The comparison between the LMM and the period 1981–2010 indicates that winter and summer were the seasons with the largest circulation anomalies. Nevertheless, this overall picture hides important temporal variations, ranging from seasonal to decadal time scales.
- The atmospheric circulation during the LMM displayed contrasting seasonal signals. The year-round

deficit of westerlies was partially compensated by an increase of northerly and southerly winds in winter and summer, respectively. As a consequence, the winter circulation changes were prone to cold conditions, while the summer circulation tended to favor relatively warm conditions. Therefore, much of the circulation-driven LMM cooling was confined to winter.

- Despite the meridional character of the winter circulation during the LMM, this period was not exceptional when compared to more recent periods because of the presence of significant decadal variability of the North Atlantic atmospheric circulation within the LMM. Thus, our observational indices reveal that the winter decline of the westerlies was accompanied by an increase in northerly winds and hence colder winters in the first half of the LMM, but by enhanced southerlies and mild winters in the second half of the LMM.

- To assess the role of the dynamics in explaining the LMM winter cooling, we derived the temperature conditions from the circulation of each winter and compared them with independent evidences. This is a substantial step forward toward a better understanding of the LMM and an important novelty with respect to previous studies. The results add observational support to the majority of extremely cold winters documented in the literature, but additionally show considerable interannual variability and spatial heterogeneity. Thus, our dynamical-based approach suggests the existence of relatively cold winters, as well as a considerable number of mild winters. In addition, some of the winters that have been previously classified as cold at continental scales may have displayed more heterogeneous patterns than previously thought. Our results call for caution when generalizing to European-scale temperature anomalies obtained from local records, and also highlight the added value of daily records when dealing with extreme events.

- We provide evidences of nonstationary spatial signatures of the winter NAO during the LMM. Our findings suggest that the extremely cold winters documented in the literature were dominated by a negative phase of the NAO. However, other relatively cold winters were rather characterized by a departure of the NAO dipole from zonality, probably explaining their more unnoticed cooling. These high and low zonal regimes of the NAO denote a seesaw coupling with the persistence of westerlies and have been reported for other periods of the past (e.g., Barriopedro et al. 2014), calling for caution when reconstructing the NAO from indirect proxies.

- Finally, our results stress the potential of direct marine observations over the Atlantic in providing insights

into the European climate and its variability. Thus, in addition to recurrent circulation anomalies over land (e.g., enhanced Siberian High; Luterbacher et al. 2001), our findings indicate large departures over the North Atlantic, in agreement with the hypothesis of an anomalous blocking activity (Barriopedro et al. 2008). The promising outcomes of this study will hopefully stimulate future studies using these historical data to characterize past climate.

REFERENCES

Alcoforado, M.-J., M. de Fátima Nunes, J. C. Garcia, and J. P. Taborda, 2000: Temperature and precipitation reconstruction in southern Portugal during the Late Maunder Minimum (AD 1675–1715). *Holocene*, **10**, 333–340, https://doi.org/10.1191/095968300674442959.

Andres, H. J., and W. R. Peltier, 2016: Regional influences of natural external forcings on the transition from the Medieval Climate Anomaly to the Little Ice Age. *J. Climate*, **29**, 5779–5800, https://doi.org/10.1175/JCLI-D-15-0599.1.

Ayre, M., J. Nicholls, C. Ward, and D. Wheeler, 2015: Ships' logbooks from the Arctic in the pre-instrumental period. *Geosci. Data J.*, **2**, 53–62, https://doi.org/10.1002/gdj3.27.

Barboza, L., B. Li, M. P. Tingley, and F. G. Viens, 2014: Reconstructing past temperatures from natural proxies and estimated climate forcings using short- and long-memory models. *Ann. Appl. Stat.*, **8**, 1966–2001, https://doi.org/10.1214/14-AOAS785.

Barnston, A. G., and R. E. Livezey, 1987: Classification, seasonality and persistence of low-frequency atmospheric circulation patterns. *Mon. Wea. Rev.*, **115**, 1083–1126, https://doi.org/10.1175/1520-0493(1987)115<1083:CSAPOL>2.0.CO;2.

Barriopedro, D., R. García-Herrera, and R. Huth, 2008: Solar modulation of Northern Hemisphere winter blocking. *J. Geophys. Res.*, **113**, D14118, https://doi.org/10.1029/2008JD009789.

——, D. Gallego, M. C. Álvarez-Castro, R. García-Herrera, D. Wheeler, C. Peña-Ortiz, and S. M. Barbosa, 2014: Witnessing North Atlantic westerlies variability from ships' logbooks (1685–2008). *Climate Dyn.*, **43**, 939–955, https://doi.org/10.1007/s00382-013-1957-8.

Brázdil, R., T. Černušák, and L. Řezníčková, 2008: Weather information in the diaries of the Premonstratensian Abbey at Hradisko, in the Czech Republic, 1693–1783. *Weather*, **63**, 201–207, https://doi.org/10.1002/wea.264.

Camuffo, D., and Coauthors, 2010: 500-year temperature reconstruction in the Mediterranean Basin by means of documentary data and instrumental observations. *Climatic Change*, **101**, 169–199, https://doi.org/10.1007/s10584-010-9815-8.

Cattiaux, J., R. Vautard, C. Cassou, P. Yiou, V. Masson-Delmotte, and F. Codron, 2010: Winter 2010 in Europe: A cold extreme in a warming climate. *Geophys. Res. Lett.*, **37**, L20704, https://doi.org/10.1029/2010GL044613.

Chambers, F. M., S. A. Brain, D. Mauquoy, J. McCarroll, and T. Daley, 2014: The "Little Ice Age" in the Southern Hemisphere in the context of the last 3000 years: Peat-based proxy-climate data from Tierra del Fuego. *Holocene*, **24**, 1649–1656, https://doi.org/10.1177/0959683614551232.

Compo, G. P., and Coauthors, 2011: The Twentieth Century Reanalysis Project. *Quart. J. Roy. Meteor. Soc.*, **137**, 1–28, https://doi.org/10.1002/qj.776.

Cornes, R. C., P. D. Jones, K. R. Briffa, and T. J. Osborn, 2013: Estimates of the North Atlantic Oscillation back to 1692 using a Paris-London westerly index. *Int. J. Climatol.*, **33**, 228–248, https://doi.org/10.1002/joc.3416.

D'Arrigo, R., R. Wilson, and G. Jacoby, 2006: On the long-term context for late twentieth century warming. *J. Geophys. Res.*, **111**, D03103, https://doi.org/10.1029/2005JD006352.

Derham, W., 1708: The history of the great frost in the last winter 1703 and 1708/9. *Philos. Trans. Roy. Soc.*, **26**, 453–478, https://doi.org/10.1098/rstl.1708.0073.

Fernández-Donado, L., and Coauthors, 2013: Large-scale temperature response to external forcing in simulations and reconstructions of the last millennium. *Climate Past*, **9**, 393–421, https://doi.org/10.5194/cp-9-393-2013.

Freeman, E., and Coauthors, 2017: ICOADS release 3.0: A major update to the historical marine climate record. *Int. J. Climatol.*, **37**, 2211–2232, https://doi.org/10.1002/joc.4775.

Gallego, D., R. García-Herrera, N. Calvo, and P. Ribera, 2007: A new meteorological record for Cádiz (Spain) 1806–1852: Implications for climatic reconstructions. *J. Geophys. Res.*, **112**, D12108, https://doi.org/10.1029/2007JD008517.

——, P. Ordóñez, P. Ribera, C. Peña-Ortiz, and R. García-Herrera, 2015: An instrumental index of the West African monsoon back to the nineteenth century. *Quart. J. Roy. Meteor. Soc.*, **141**, 3166–3176, https://doi.org/10.1002/qj.2601.

Garcia, R. R., and Coauthors, 2001: Atmospheric circulation changes in the tropical Pacific inferred from the voyages of the Manila galleons in the sixteenth–eighteenth centuries. *Bull. Amer. Meteor. Soc.*, **82**, 2435–2455, https://doi.org/10.1175/1520-0477(2001)082<2435:ACCITT>2.3.CO;2.

Gómez-Navarro, J. J., E. Zorita, C. C. Raible, and R. Neukom, 2017: Pseudo-proxy tests of the analogue method to reconstruct spatially resolved global temperature during the Common Era. *Climate Past*, **13**, 629–648, https://doi.org/10.5194/cp-13-629-2017.

Goosse, H., E. Crespin, S. Dubinkina, M.-F. Loutre, M. E. Mann, H. Renssen, Y. Sallaz-Damaz, and D. Shindell, 2012: The role of forcing and internal dynamics in explaining the "Medieval Climate Anomaly." *Climate Dyn.*, **39**, 2847–2866, https://doi.org/10.1007/s00382-012-1297-0.

Harris, I., P. D. Jones, T. J. Osborn, and D. H. Lister, 2014: Updated high-resolution grids of monthly climatic observations—The CRU TS3.10 dataset. *Int. J. Climatol.*, **34**, 623–642, https://doi.org/10.1002/joc.3711.

Hegerl, G., J. Luterbacher, F. González-Rouco, S. F. B. Tett, T. Crowley, and E. Xoplaki, 2011: Influence of human and natural forcing on European seasonal temperatures. *Nat. Geosci.*, **4**, 99–103, https://doi.org/10.1038/ngeo1057.

Hurrell, J. W., 1995: Decadal trends in the North Atlantic Oscillation: Regional temperatures and precipitation. *Science*, **269**, 676–679, https://doi.org/10.1126/science.269.5224.676.

——, Y. Kushnir, G. Ottersen, and M. Visbeck, 2003. An overview of the North Atlantic Oscillation. *The North Atlantic Oscillation: Climatic Significance and Environmental Impact*, Geophys. Monogr., Vol. 134, Amer. Geophy. Union, 1–35.

Jackson, A., A. R. T. Jonkers, and M. R. Walker, 2000: Four centuries of geomagnetic secular variation from historical records. *Philos. Trans. Roy. Soc.*, **358A**, 957–990, https://doi.org/10.1098/rsta.2000.0569.

Jones, P. D., and M. Salmon, 2005: Preliminary reconstructions of the North Atlantic Oscillation and the Southern Oscillation index from measures of wind strength and direction taken during the CLIWOC period. *Climatic Change*, **73**, 131–154, https://doi.org/10.1007/s10584-005-6948-2.

——, T. Jonsson, and D. Wheeler, 1997: Extension to the North Atlantic Oscillation using early instrumental pressure observations from Gibraltar and south-west Iceland. *Int. J. Climatol.*, **17**, 1433–1450, https://doi.org/10.1002/(SICI)1097-0088(19971115)17:13<1433::AID-JOC203>3.0.CO;2-P.

——, C. Harpham, and B. M. Vinther, 2014: Winter-responding proxy temperature reconstructions and the North Atlantic Oscillation. *J. Geophys. Res. Atmos.*, **119**, 6497–6505, https://doi.org/10.1002/2014JD021561.

Kaufman, D., 2014: A community-driven framework for climate reconstructions. *Eos, Trans. Amer. Geophys. Union*, **95**, 361–363, https://doi.org/10.1002/2014EO400001.

Kidston, J., A. A. Scaife, S. C. Hardiman, D. M. Mitchell, N. Butchart, M. P. Baldwin, and L. J. Gray, 2015: Stratospheric influence on tropospheric jet streams, storm tracks and surface weather. *Nat. Geosci.*, **8**, 433–440, https://doi.org/10.1038/ngeo2424.

Kington, J., 2010: *Climate and Weather*. Harper Collins Publishers, 484 pp.

Küttel, M., and Coauthors, 2010: The importance of ship log data: Reconstructing North Atlantic, European and Mediterranean sea level pressure fields back to 1750. *Climate Dyn.*, **34**, 1115–1128, https://doi.org/10.1007/s00382-009-0577-9.

——, J. Luterbacher, and H. Wanner, 2011: Multidecadal changes in winter circulation-climate relationship in Europe: Frequency variations, within-type modifications, and long-term trends. *Climate Dyn.*, **36**, 957–972, https://doi.org/10.1007/s00382-009-0737-y.

Lamb, H. H., 1972: *British Isles Weather Types and a Register of the Daily Sequence of Circulation Patterns, 1861–1971*. Geophysical Memoir 116, HMSO, 85 pp.

Landrum, L., B. L. Otto-Bliesner, E. R. Wahl, A. Conley, P. J. Lawrence, N. Rosenbloom, and H. Teng, 2013: Last millennium climate and its variability in CCSM4. *J. Climate*, **26**, 1085–1111, https://doi.org/10.1175/JCLI-D-11-00326.1.

Lawrimore, J. H., M. J. Menne, B. E. Gleason, C. N. Williams, D. B. Wuertz, R. S. Vose, and J. Rennie, 2011: An overview of the Global Historical Climatology Network monthly mean temperature data set, version 3. *J. Geophys. Res.*, **116**, D19121, https://doi.org/10.1029/2011JD016187.

Lehner, F., A. Born, C. C. Raible, and T. F. Stocker, 2013: Amplified inception of European Little Ice Age by sea ice–ocean–atmosphere feedbacks. *J. Climate*, **26**, 7586–7602, https://doi.org/10.1175/JCLI-D-12-00690.1.

Ljungqvist, F. C., P. J. Krusic, G. Brattström, and H. S. Sundqvist, 2012: Northern Hemisphere temperature patterns in the last 12 centuries. *Climate Past*, **8**, 227–249, https://doi.org/10.5194/cp-8-227-2012.

Luterbacher, J., and C. Pfister, 2015: The year without a summer. *Nat. Geosci.*, **8**, 246–248, https://doi.org/10.1038/ngeo2404.

——, R. Rickli, E. Xoplaki, C. Tinguely, C. Beck, C. Pfister, and H. Wanner, 2001: The Late Maunder Minimum (1675–1715)—A key period for studying decadal scale climatic change in Europe. *Climatic Change*, **49**, 441–462, https://doi.org/10.1023/A:1010667524422.

——, D. Dietrich, E. Xoplaki, M. Grosjean, and H. Wanner, 2004: European seasonal and annual temperature variability, trends, and extremes since 1500. *Science*, **303**, 1499–1503, https://doi.org/10.1126/science.1093877.

Manley, G., 1974: Central England temperatures: Monthly means 1659 to 1973. *Quart. J. Roy. Meteor. Soc.*, **100**, 389–405, https://doi.org/10.1002/qj.49710042511.

Mann, M. E., and Coauthors, 2009: Global signatures and dynamical origins of the Little Ice Age and Medieval Climate Anomaly. *Science*, **326**, 1256–1260, https://doi.org/10.1126/science.1177303.

Maraldi, J.-P., 1710: Sur les arbres morts par la gelee de 1709. Histoire de l'Académie Royale des Sciences, 59–61.

Masson-Delmotte, V., and Coauthors, 2013: Information from paleoclimate archives. *Climate Change 2013: The Physical Science Basis*, T. F. Stocker et al., Eds., Cambridge University Press, 383–464, https://doi.org/10.1017/CBO9781107415324.

McShane, B. B., and A. J. Wyner, 2011: A statistical analysis of multiple temperature proxies: Are reconstructions of surface temperatures over the last 1000 years reliable? *Ann. Appl. Stat.*, **5**, 5–44, https://doi.org/10.1214/10-AOAS398.

Menne, M. J., I. Durre, R. S. Vose, B. E. Gleason, and T. G. Houston, 2012: An overview of the Global Historical Climatology Network-Daily database. *J. Atmos. Oceanic Technol.*, **29**, 897–910, https://doi.org/10.1175/JTECH-D-11-00103.1.

Monahan, W. G., 1993: *Year of Sorrows: The Great Famine of 1709 in Lyon*. Ohio State University Press, 256 pp.

Niedźwiedź, T., 2010: Summer temperatures in the Tatra Mountains during the Maunder Minimum (1645–1715). The Polish Climate in the European Context: An Historical Overview, R. Przybylak et al., Eds., Springer, 397–406, https://doi.org/10.1007/978-90-481-3167-9.

Ordóñez, P., D. Gallego, P. Ribera, C. Peña-Ortiz, and R. García-Herrera, 2016: Tracking the Indian summer monsoon onset back to the preinstrument period. *J. Climate*, **29**, 8115–8127, https://doi.org/10.1175/JCLI-D-15-0788.1.

Ouzeau, G., J. Cattiaux, H. Douville, A. Ribes, and D. Saint-Martin, 2011: European cold winter 2009–2010: How unusual in the instrumental record and how reproducible in the ARPEGE-Climat model? *Geophys. Res. Lett.*, **38**, L11706, https://doi.org/10.1029/2011GL047667.

PAGES 2k Consortium, 2013: Continental-scale temperature variability during the past two millennia. *Nat. Geosci.*, **6**, 339–346, https://doi.org/10.1038/ngeo1797.

Pauling, A., J. Luterbacher, C. Casty, and H. Wanner, 2006: Five hundred years of gridded high-resolution precipitation reconstructions over Europe and the connection to large-scale circulation. *Climate Dyn.*, **26**, 387–405, https://doi.org/10.1007/s00382-005-0090-8.

Pfister, C., 1992: Monthly temperature and precipitation in central Europe from 1525–1979: Quantifying documentary evidence on weather and its effect. *Climate since A.D. 1500*, R. S. Bradley and P. D. Jones, Eds., Routledge, 118–142.

Prior, J., and M. Kendon, 2011: The UK winter of 2009/2010 compared with severe winters of the last 100 years. *Weather*, **66**, 4–10, https://doi.org/10.1002/wea.735.

Rácz, L., 1994: The climate of Hungary during the Late Maunder Minimum (1675–1715). *Climatic Trends and Anomalies in Europe 1675–1715*, B. Frenzel, C. Pfister, and B. Gläser, Eds., G. Fischer, 43–50.

Rhodes, R. H., N. A. N. Bertler, J. A. Baker, H. C. Steen-Larsen, S. B. Sneed, U. Morgenstern, and S. J. Johnsen, 2012: Little Ice Age climate and oceanic conditions of the Ross Sea, Antarctica from a coastal ice core record. *Climate Past*, **8**, 1223–1238, https://doi.org/10.5194/cp-8-1223-2012.

Schamm, K., M. Ziese, A. Becker, P. Finger, A. Meyer-Christoffer, U. Schneider, M. Schröder, and P. Stender, 2014: Global gridded precipitation over land: A description of the new GPCC First Guess Daily product. *Earth Syst. Sci. Data*, **6**, 49–60, https://doi.org/10.5194/essd-6-49-2014.

Schimanke, S., H. E. M. Meier, E. Kjellström, G. Strandberg, and R. Hordoir, 2012: The climate in the Baltic Sea region during the last millennium simulated with a regional climate model. *Climate Past*, **8**, 1419–1433, https://doi.org/10.5194/cp-8-1419-2012.

Schurer, A. P., G. C. Hegerl, M. E. Mann, S. F. B. Tett, and S. J. Phipps, 2013: Separating forced from chaotic climate variability over the past millennium. *J. Climate*, **26**, 6954–6973, https://doi.org/10.1175/JCLI-D-12-00826.1.

Slonosky, V. C., P. D. Jones, and T. D. Davies, 2001: Instrumental pressure observations and atmospheric circulation from the 17th and 18th centuries: London and Paris. *Int. J. Climatol.*, **21**, 285–298, https://doi.org/10.1002/joc.611.

Trigo, R. M., J. M. Vaquero, M.-J. Alcoforado, M. Barriendos, J. Taborda, R. García-Herrera, and J. Luterbacher, 2009: Iberia in 1816, the year without a summer. *Int. J. Climatol.*, **29**, 99–115, https://doi.org/10.1002/joc.1693.

Van den Dool, H. M., H. J. Krijnen, and C. J. E. Schuurmans, 1978: Average winter temperatures at De Bilt (the Netherlands): 1634–1977. *Climatic Change*, **1**, 319–330, https://doi.org/10.1007/BF00135153.

Vaquero, J. M., and Coauthors, 2016: A revised collection of sunspot group numbers. *Sol. Phys.*, **291**, 3061–3074, https://doi.org/10.1007/s11207-016-0982-2.

Vautard, R., and P. Yiou, 2009: Control of recent European surface climate change by atmospheric flow. *Geophys. Res. Lett.*, **36**, L22702, https://doi.org/10.1029/2009GL040480.

——, and ——, 2012: Attribution: Robustness of warming attribution. *Nat. Climate Change*, **2**, 26–27, https://doi.org/10.1038/nclimate1343.

Vega, I., D. Gallego, P. Ribera, F. de Paula Gómez-Delgado, R. García-Herrera, and C. Peña-Ortiz, 2018: Reconstructing the western North Pacific summer monsoon since the late nineteenth century. *J. Climate*, **31**, 355–368, https://doi.org/10.1175/JCLI-D-17-0336.1.

Vicente-Serrano, S. M., and Coauthors, 2016: The westerly index as complementary indicator of the North Atlantic Oscillation in explaining drought variability across Europe. *Climate Dyn.*, **47**, 845–863, https://doi.org/10.1007/s00382-015-2875-8.

Wanner, H., and Coauthors, 1995: Wintertime European circulation patterns during the Late Maunder Minimum cooling period (1675–1704). *Theor. Appl. Climatol.*, **51**, 167–175, https://doi.org/10.1007/BF00867443.

——, H. P. Holzhauser, C. Pfister, and H. Zumbühl, 2000: Interannual to century scale climate variability in the European Alps. *Erdkunde*, **54**, 62–69, https://doi.org/10.3112/erdkunde.2000.01.05.

Wheeler, D., 2005: British naval logbooks from the late seventeenth century: New climatic information from old sources. *Hist. Meteor.*, **2**, 133–146.

——, 2014: Hubert Lamb's 'treasure trove': Ships' logbooks in climate research. *Weather*, **69**, 133–139, https://doi.org/10.1002/wea.2284.

——, and R. García-Herrera, 2008: Ships' logbooks in climatological research. *Ann. N. Y. Acad. Sci.*, **1146**, 1–15, https://doi.org/10.1196/annals.1446.006.

——, ——, C. W. Wilkinson, and C. Ward, 2010: Atmospheric circulation and storminess derived from Royal Navy logbooks: 1685 to 1750. *Climatic Change*, **101**, 257–280, https://doi.org/10.1007/s10584-009-9732-x.

Wilks, D. S., 2006: *Statistical Methods in the Atmospheric Sciences*. 2nd ed. Elsevier, 627 pp.

Xoplaki, E., P. Maheras, and J. Luterbacher, 2001: Variability of climate in meridional Balkans during the periods 1675–1715 and 1780–1830 and its impact on human life. *Climatic Change*, **48**, 581–615, https://doi.org/10.1023/A:1005616424463.

——, J. Luterbacher, H. Paeth, D. Dietrich, N. Steiner, M. Grosjean, and H. Wanner, 2005:European spring and autumn temperature variability and change of extremes over the last half millennium, *Geophys. Res. Lett.*, **32**, L15713, https://doi.org/10.1029/2005GL023424.